Nonlinear Models of Reinforced and Post-tensioned Concrete Beams

P. Fanning

Lecturer, Department of Civil Engineering, University College Dublin
Earlsfort Terrace, Dublin 2, Ireland.
Email: paul.fanning@ucd.ie

Received 16 Jul 2001; revised 8 Sep 2001; accepted 12 Sep 2001.

ABSTRACT

Commercial finite element software generally includes dedicated numerical models for the nonlinear response of concrete under loading. These models usually include a smeared crack analogy to account for the relatively poor tensile strength of concrete, a plasticity algorithm to facilitate concrete crushing in compression regions and a method of specifying the amount, the distribution and the orientation of any internal reinforcement. The numerical model adopted by ANSYS is discussed in this paper. Appropriate numerical modelling strategies are recommended and comparisons with experimental load-deflection responses are discussed for ordinary reinforced concrete beams and post-tensioned concrete T-beams.

KEYWORDS

Concrete; post-tensioning; finite element modelling.

1. Introduction: the ANSYS reinforced concrete model

The implementation of nonlinear material laws in finite element analysis codes is generally tackled by the software development industry in one of two ways. In the first instance the material behaviour is programmed independently of the elements to which it may be specified. Using this approach the choice of element for a particular physical system is not limited and best practice modelling techniques can be used in identifying an appropriate element type to which any, of a range, of nonlinear material properties are assigned. This is the most versatile approach and does not limit the analyst to specific element types in configuring the problem of interest. Notwithstanding this however certain software developers provide specific specialised nonlinear material capabilities only with dedicated element types. ANSYS [1] provides a dedicated three-dimensional eight noded solid isoparametric element, Solid65, to model the nonlinear response of brittle materials based on a constitutive model for the triaxial behaviour of concrete after Williams and Warnke [2].

The element includes a smeared crack analogy for cracking in tension zones and a plasticity algorithm to account for the possibility of concrete crushing in compression zones. Each element has eight integration points at which cracking and crushing checks are performed. The element behaves in a linear elastic manner until either of the specified tensile or compressive strengths are exceeded. Cracking or crushing of an element is initiated once one of the element principal stresses, at an element integration point, exceeds the tensile or compressive strength of the concrete. Cracked or crushed regions, as opposed to discrete cracks, are then formed perpendicular to the relevant principal stress direction with stresses being redistributed locally. The element is thus nonlinear and requires an iterative solver. In the numerical routines the formation of a crack is achieved by the modification of the stress-strain relationships of the element to introduce a plane of weakness in the requisite principal stress direction. The amount of shear transfer across a crack can be varied between full shear transfer and no shear transfer at a cracked section. The crushing algorithm is akin to a plasticity law in that the once a section has crushed any further application of load in that direction develops increasing strains at constant stress. Subsequent to the formation of an initial crack, stresses tangential to the crack face may cause a second, or third, crack to develop at an integration point.

The internal reinforcement may be modelled as an additional smeared stiffness distributed through an element in a specified orientation or alternatively by using discrete strut or beam elements connected to the solid elements. The beam elements would allow the internal reinforcement to develop shear stresses but as these elements, in ANSYS, are linear no plastic deformation of the reinforcement is possible. The smeared stiffness and link modelling options allow the elastic-plastic response of the reinforcement to be included in the simulation at the expense of the shear stiffness of the reinforcing bars.

2. Test case beams

Results of ultimate load tests on ordinarily reinforced and post-tensioned concrete beams were used to assess the suitability of the reinforced concrete model implemented in ANSYS in predicting the ultimate response of reinforced concrete beams.

- *3.0m long Ordinarily Reinforced Concrete Beams*

A cross section through the 3.0m long beams, Figure 1, illustrates the internal reinforcement. Three 12mm diameter steel bars were included in the tension zone with two 12mm steel bars as compression steel. Ten shear links, formed from 6mm mild steel bars, were provided at 125mm centres for shear reinforcement in the shear spans. Two beams were tested each of which were simply supported with a clear span of 2.8m and loaded symmetrically and monotonically, under displacement control, in four point bending, with point loads 0.3m either side of the mid-span location, to failure. Cylinder splitting [3] and crushing tests [4] on cored samples of the beams, in accordance with the British Standards, were undertaken to identify the uni-axial tensile and compressive strengths of the concrete, (f_t = 5.1N/mm^2 and f_c = 69.0N/mm^2 respectively), and the Young's Modulus of the concrete [5], (39,200 N/mm^2), for inclusion in the numerical models. Tensile tests on samples of the reinforcing bars and shear links were also undertaken such that their nonlinear plastic response could be accurately simulated in the numerical models.

- *9.0m long Third Scale Prestressed Beams* [6]

A cross section and elevation of third scale models of 30m long prestressed concrete beams tested at the Slovenian National Building and Civil Engineering Institute, Ljubljana, Slovenia are shown in Figure 2. The flange of the T-beam is 1.1m wide and 0.08m deep while the web is effectively an I-beam with a flange width of 0.29m and an overall depth of 0.6m. In addition to ordinary reinforcing bars, three grouted 0.6" (15.2 mm) tendons, each composed of 7×5.08 mm diameter wires, were used to post-tension each beam. Tensile tests on the reinforcing bars and tendons and strength and stiffness tests on the concrete identified the relevant material properties, linear and nonlinear, for the numerical model.

The beam was loaded to failure while deflection and strain data, on the external concrete surfaces and on the individual cables, were monitored. The load arrangement is illustrated in Figure 3 and in all cases the uniformly distributed loading was applied initially with the point loads P1 and P2 being applied in subsequent increments until the ultimate load of the beam was reached.

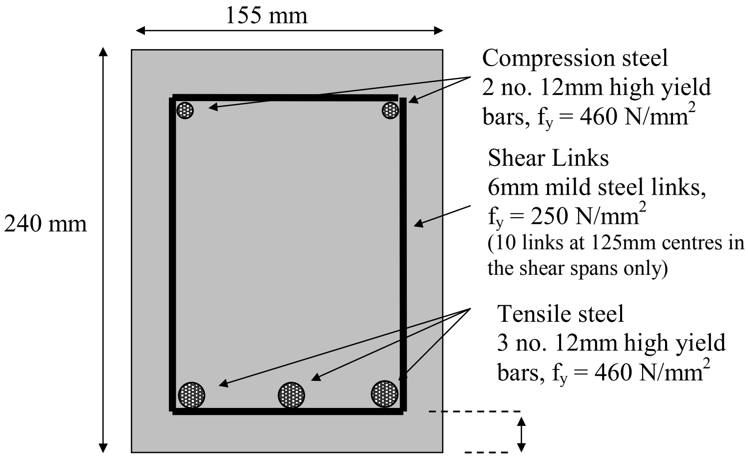

Figure 1: Cross section details for the 3.0m beams

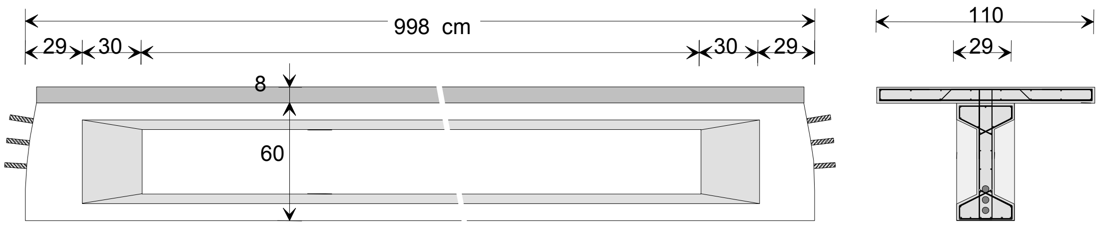

Figure 2: Elevation and cross-section of the model post-tensioned beam

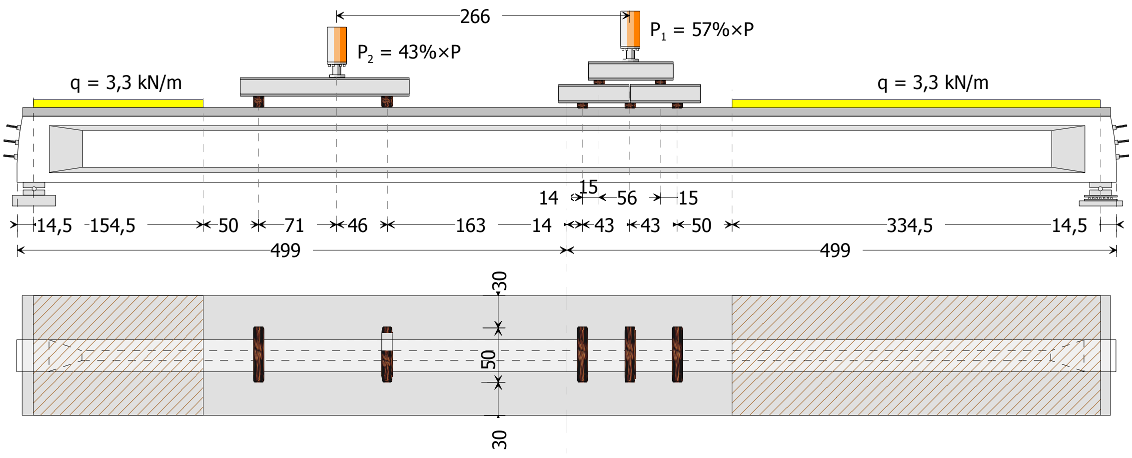

Figure 3: Loading arrangement

3. Finite element modeling strategies

The requirement to include the nonlinear response of reinforced concrete in capturing the ultimate response of both the post-tensioned and ordinarily reinforced beams demands the use of the dedicated Solid65 element in ANSYS. The existence of symmetry planes, two for the 3.0m beams and one for the prestressed beams, resulted in only quarter and half models being required respectively. The finite element mesh for the 3.0m beams is plotted in Figure 4 with the mesh for the prestressed beams shown in Figure 5.

The internal reinforcement for the 3.0m beams were modelled using three dimensional spar elements with plasticity, Link8, embedded within the solid mesh. This option was favoured over the alternative smeared stiffness capability as it allowed the reinforcement to be precisely located whilst maintaining a relatively coarse mesh for the surrounding concrete medium. The inherent assumption is that there is full displacement compatibility between the reinforcement and the concrete and that no bond slippage occurs. The model was loaded, through applied displacement to facilitate easier convergence, in a manner consistent with the test programme.

In formulating the model for the post-tensioned beams the three dimensional spar elements with plasticity, Link8, were employed for the post-tensioning cables (primary reinforcement), with the remaining internal reinforcing bars modelled using the alternative distributed smeared stiffness approach. The post-tensioning was modelled via an initial strain in the tendon elements, corresponding to tendon tensile forces, in a preliminary load stage. Subsequently the uniformly distributed loading was specified in a second load stage prior to the model being loaded to failure in a third solution stage in a manner consistent with the test data.

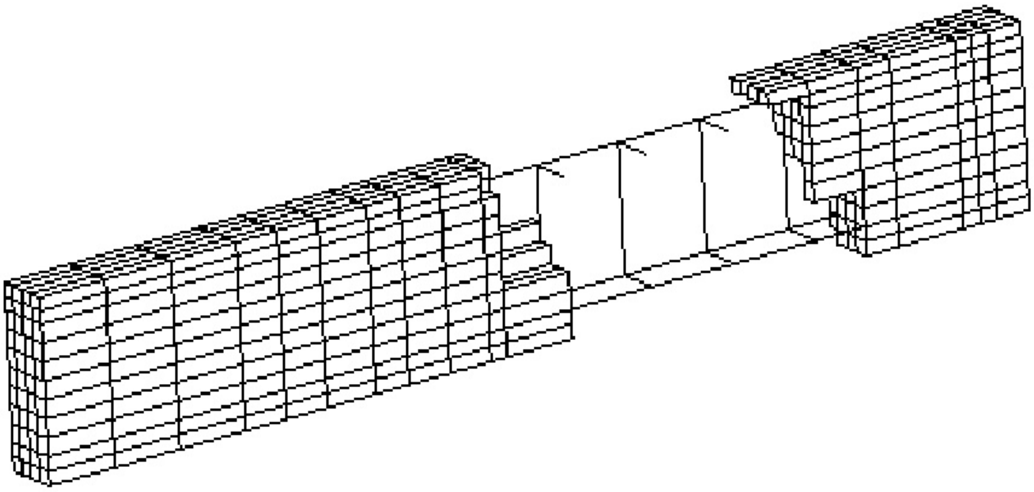

Figure 4: 3.0m beams – finite element mesh (selected concrete elements removed to illustrate internal reinforcement)

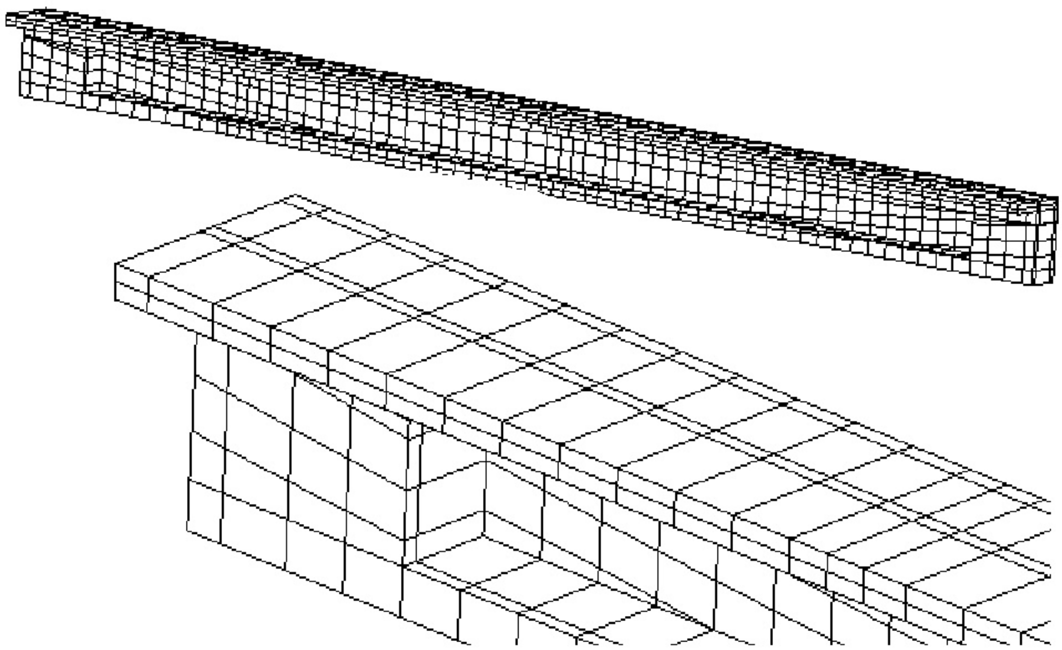

Figure 5: Post-tensioned beams – finite element mesh

4. Comparison of experimental and numerical results

The load deflection responses for the 3.0m beams, from the test programme, are plotted with the finite element results in Figure 6. The numerical model predicts an ultimate load of 66.1kN and captures well the nonlinear load deflection response of the beams up to failure. The ultimate loads reached in the tests were 66.18kN and 66.7kN respectively. It is clear form the numerical model that the response of the model is linear until the first crack has formed at approximately 17kN. Although the measured response of the beams were, initially, slightly less stiff the first visible crack appeared at approximately 17kN also. Beyond this point the almost linear response of the finite element model is consistent with the test data. Classical reinforced concrete theory [7], predicted tensile reinforcement yielding to commence at approximately 59kN which is consistent with the change in slope of the load deflection response for both the test and numerical beams.

The ultimate midspan deflection of the 3.0m beams recorded in the tests was of the order of 45mm. In the numerical model the increased plastic deformation in the internal reinforcement was such that converged solutions were not achieved beyond about 27mm deflection at midspan. The experimental crack distribution at midspan (left-hand side of beam shown) and the crack distribution, predicted by the FE model (right-hand side), are illustrated in Figure 7. The FE model predicts that flexural cracks, formed at ninety degrees to the dashes, extend uniformly through the depth of the beam before becoming less uniform as the compression face is approached. This is also evident in the test beam. However the discrete nature of the flexural cracks is not captured using a smeared crack model. The mode of failure predicted using the numerical model was a flexural mode of failure, consistent with the test response, due to increasing plastic strains developed in the tension reinforcement.

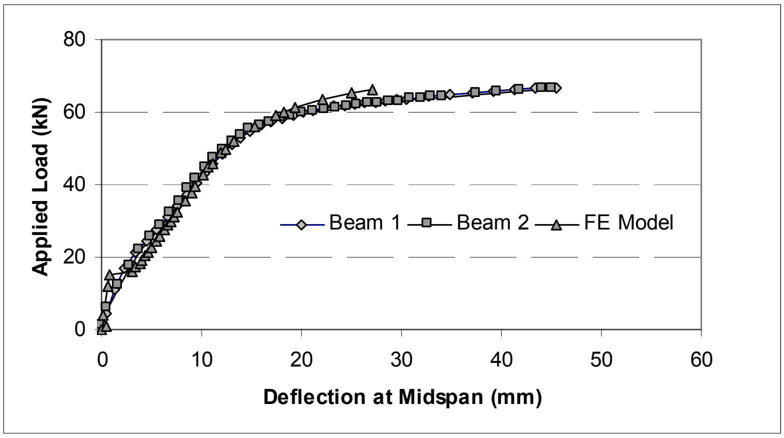

Figure 6: 3.0m Beams - Experimental and FE load deflection responses

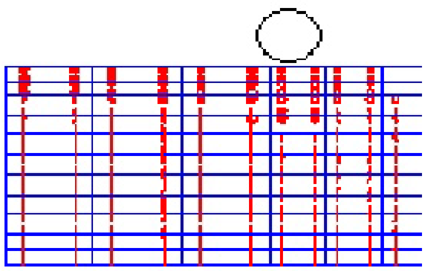

Numerical smeared cracks formed parallel to vertical dashed lines

Figure 7: **Test and FE crack distributions at failure**

The load deflection response for the post-tensioned T-beams is captured accurately by the numerical simulation (see Figure 8). The ultimate load achieved in the numerical model, 231kN, is within 12% of the ultimate test load of 264kN. The concrete strains measured during testing on the top and bottom faces of the beam during testing are compared to the numerical results in Figure 9. The correlation between test and numerical data is again good up to the 1% strain limit of the strain gauges used in the test programme.

The mode of failure in the test beam was a flexural mode with the neutral axis rising through the section as the yield strength of the post-tensioning cables and the internal reinforcement was reached and eventually exceeded. Although the strains predicted by the numerical model were slightly lower than those measured in the test programme the manner of failure was the same with the numerical model becoming unstable as flexural cracks propagated through the depth of the beam as the stress and strain in the tendons and reinforcement increased.

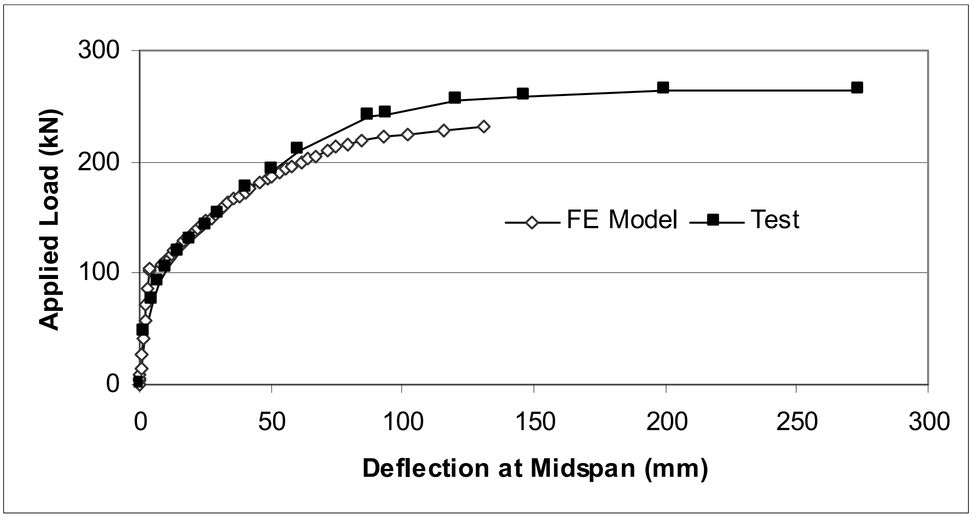

Figure 8: Post-tensioned - Experimental and FE load deflection responses

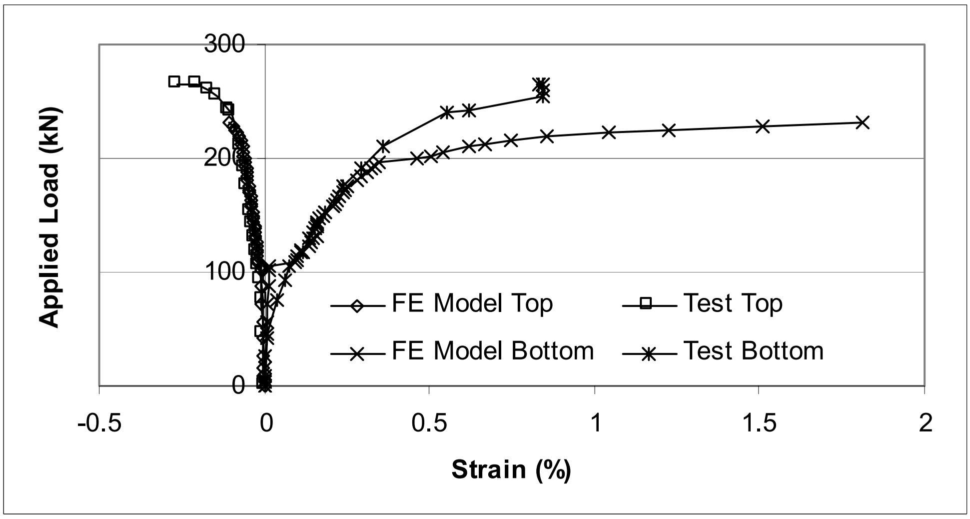

Figure 9: Post-tensioned - Experimental and FE load deflection responses

5. Discussion

The numerical models for both the 3.0m ordinarily reinforced beams and the post-tensioned beams were consistent with the test results in both cases. Clearly the correlation of test and numerical data depends on the assignment of accurate linear and non-linear material properties as appropriate. Generally concrete crushing tests undertaken for concrete samples of new structures and cores, for the same purpose, are usually taken when assessing existing structures. Cylinder splitting tests for tensile strength and stiffness tests for Young's modulus measurements are generally more complex and it is instructive to assess existing rules of thumb for assessing both concrete tensile strength and Young's modulus in order that numerical modelling methodologies can be universally applied.

Hughes [8] proposed that the Young's modulus of concrete is related to its compressive strength by:

$$E_c = 9100\,(f_{cu})^{1/3}$$

In this case Hughes [8] yields a Young's modulus of 37,324N/mm^2 which is within 5% of the averaged measured value of 39,200N/mm^2.

The British Standard for reinforced concrete [9] estimates the tensile strength of concrete from its known compression strength by;

$$f_t = 0.36\,(f_{cu})^{1/2}$$

and predicts a tensile strength of 2.99N/mm^2 for a concrete with cube strength, f_{cu} = 69 N/mm^2. Using cylinder splitting tests the measured value of the tensile strength of the concrete was 5.1N/mm^2. Although significantly lower than the measured tensile strength of the concrete the effect on the prediction of the ultimate response of the beam is small as the concrete invariably cracks forcing the reinforcement to carry any tensile stresses.

In general given the compressive strength of the concrete it is thus usually possible to arrive at a sensible set of material data for inclusion in the nonlinear numerical model. The situation is not as clear in the context of the reinforcing bars. Generally the nominal strength of the reinforcement is specified and it is assumed in design that it behaves in an elastic-perfectly plastic manner. Tensile tests on the high strength steel reinforcement (nominal σ_y = 460 N/mm^2) gave a Young's modulus of 204,000N/mm^2 and a 0.2% proof stress of 532.4N/mm^2. A load deflection response with generic material properties based on the measured compressive strength of the concrete and nominal yield strength of the reinforcement is included with the FE Model results and experimental results in Figure 10.

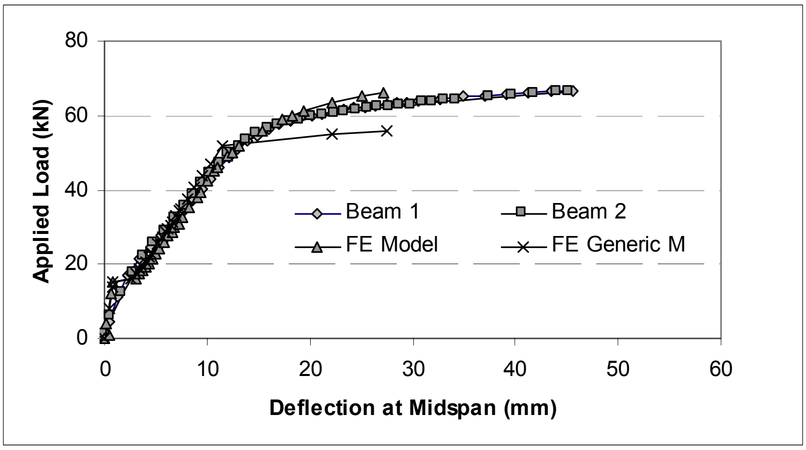

Figure 10: 3.0m Beams – Sensitivity of load deflection responses to material properties

The FE model with generic material properties is seen to underestimate the strength of the reinforced concrete beam. The ultimate load predicted is approximately 55.8kN compared to 66kN achieved in the test programme. The difference in ultimate load is approximately equal to the ratio between the assumed and measured yield strength of the reinforcement.

The results of both finite element models were found to be particularly sensitive to the Young's modulus of the concrete and the yield strength of the reinforcement. For both the 3.0m beams and the post-tensioned beams the Young's modulus derived from testing agreed with the predictions by Hughes [8] thus leaving the yield strength of the reinforcement, and post-tensioning cables, as the critical parameter in identifying accurately the ultimate loads of the beams. In respect of the post-tensioned beams the ultimate load is also dependent on the actual level of post-tensioning.

6. Conclusions

Finite element models of 3.0m ordinarily reinforced concrete beams and 9.0m post-tensioned concrete beams, constructed in ANSYS V5.5 using the dedicated concrete element have accurately captured the nonlinear flexural response of these systems up to failure.

The dedicated element employs a smeared crack model to allow for concrete cracking with the option of modelling the reinforcement in a distributed or discrete manner. It was found that the optimum modelling strategy, in terms of controlling mesh density and accurately locating the internal reinforcement was to model the primary reinforcing in a discrete manner. Hence for ordinary reinforced concrete beams all internal reinforcement should be modelled discretely and for post-tensioned beams the post-tensioning tendons should be modelled discretely with any other additional reinforcement modelled in a distributed manner.

In terms of using finite element models to predict the strength of existing beams the assignment of appropriate material properties is critical. It was found that for a known compressive strength of concrete, which can be measured from extracted cores, existing rules of thumb for the Young's modulus and concrete tensile strength are adequate for inclusion in the numerical models. In relation to the reinforcement the actual yield strength in tension is likely to be greater than the nominal design strength and the ultimate load of the beam will thus be underestimated. In relation to post-tensioned beams the situation is complicated further by the inevitable loss in post-tensioning forces that will occur after construction and during the lifetime of the structure and these losses should be accounted for in an assessment model of a post-tensioned system.

In conclusion the dedicated smeared crack model is an appropriate numerical model for capturing the flexural modes of failure of reinforced concrete systems. In addition it should be particularly attractive to designers when they are required to accurately predict the deflection of a reinforced concrete system, for a given load, in addition to its ultimate strength.

REFERENCES

1. ANSYS, ANSYS Manual Set, 1998, ANSYS Inc., Southpoint, 275 Technology Drive, Canonsburg, PA 15317, USA.
2. William, K.J. and Warnke, E.D. "Constitutive Model for the Triaxial Behaviour of Concrete", Proceedings of the International Association for Bridge and Structural Engineering, 1975, 19, p.174, ISMES, Bergamo, Italy
3. BS 1881, Testing Concrete, Part 117, 'Method for the Determination of Tensile Splitting Strength' , 1983, British Standards Institution, London.

4. BS 1881, Testing Concrete, Part 121, 'Method for the Determination of Compressive Strength of Concrete Cores' , 1983, British Standards Institution, London.
5. BS 1881, Testing Concrete, Part 121, 'Method for the Determination of Static Modulus of Elasticity in Compression' , 1983, British Standards Institution, London.
6. Fanning, P. and Znidaric, A., Solid Modelling of Post-Tensioned Bridge Beams using Finite Elements, to be published at fib 99 Symposium: Structural Concrete – The Bridge Between People, 1999, Prague, 12-15 October, Czech Concrete and Masonry Society.
7. O' Brien, E.J. and Dixon, A.S., Reinforced and Prestressed Concrete Design: The Complete Process, 1995, 1st Edition, Longman Scientific and Technical (UK).
8. Hughes, B.P., Limit State Theory for Reinforced Concrete Design, 1976, 2nd Edition, Pitman Publishing Ltd (London).
9. BS 8110, Structural use of Concrete, Part 1, 1985, British Standards Institution, London.